

# Charge-Density-Wave Transitions in the Local-Moment Magnet $\text{Er}_5\text{Ir}_4\text{Si}_{10}$

F. Galli,<sup>1</sup> S. Ramakrishnan,<sup>1,2</sup> T. Taniguchi,<sup>1,\*</sup> G. J. Nieuwenhuys,<sup>1</sup> J. A. Mydosh,<sup>1</sup> S. Geupel,<sup>3</sup>  
J. Lüdecke,<sup>3</sup> and S. van Smaalen<sup>3</sup>

<sup>1</sup>*Kamerlingh Onnes Laboratory, Leiden University, 2300 RA Leiden, The Netherlands*

<sup>2</sup>*Tata Institute of Fundamental Research, Mumbai-400005, India*

<sup>3</sup>*Laboratory of Crystallography, University of Bayreuth, D-95440, Bayreuth, Germany*

(Received 18 January 2000)

We report the observation of a new type of charge-density wave (CDW) in the large magnetic-moment rare-earth intermetallic compound,  $\text{Er}_5\text{Ir}_4\text{Si}_{10}$ , which then orders magnetically at low temperatures. Single crystal x-ray diffraction shows the development of a 1D incommensurate CDW at 155 K, which then locks into a purely commensurate state below 55 K. The well-localized  $\text{Er}^{3+}$  moments are antiferromagnetically ordered below 2.8 K. We observe very sharp anomalies in the specific heat at 145 and 2.8 K, signifying the bulk nature of these transitions. Our data suggest the coexistence of strongly coupled CDW with local-moment antiferromagnetism in  $\text{Er}_5\text{Ir}_4\text{Si}_{10}$ .

PACS numbers: 71.45.Lr, 75.20.Hr, 71.20.Lp

Charge-density-wave (CDW) transitions occur in low-dimensional solids where it is possible to achieve nesting of Fermi surfaces that leads to the appearance of a periodic lattice distortion with an accompanying energy gap  $\Delta$  [1–4]. These materials show striking nonlinear and anisotropic properties as well as unusual elastic and dynamic behaviors: This makes them an appealing field for experimental and theoretical studies on Fermi surface gapping and electron-phonon coupling. A number of such systems have been previously studied, including quasi-1D organic salts (e.g., TTF-TCNQ) [5] and inorganic chain compounds (e.g.,  $\text{NbSe}_3$ ) [2]. Here a Peierls–Fröhlich-type [4] phase transformation is observed at a finite temperature  $T_{\text{CDW}}$ : Above this temperature the coupled electron-phonon system is unstable with respect to a deformation of wave vector  $q = 2k_F$ . Below  $T_{\text{CDW}}$ , the ground state is characterized by a gap in the single-particle excitation spectrum.

Although many of the properties of these quasi-1D compounds could be understood within the framework of this continuous phase transition with weak electron-phonon and interchain coupling, the thermodynamic behavior of the CDW transition in compounds such as  $\text{TaSe}_2$  [6] and the blue bronzes [3] requires a description beyond the weak-coupling model. McMillan [7], using strong electron-phonon coupling and small interchain correlation lengths, was able to provide a microscopic theory, which has given a semiquantitative explanation for the peculiar behavior of these latter systems, like their specific heat jumps and  $\Delta/T_{\text{CDW}}$  ratios. In recent years interest in this area has focused on detailed investigation of these conventional CDW systems. However, in order to probe the theory further and search for novel CDW behaviors, especially those involving the interplay with magnetism, new classes of materials are needed. To the best of our knowledge there does not exist a local-moment magnet (mediated by the RKKY interaction between the  $f$  and conduction electrons) exhibiting a CDW.

We have begun a quest for new CDW systems in intermetallic rare-earth (RE) compounds and found indications in the literature [8–10] for such behavior in a series of  $\text{RE}_5\text{Ir}_4\text{Si}_{10}$  materials. Polycrystalline samples showed anomalies in the resistivity above 20 K, which were tentatively attributed to CDW or SDW (spin-density-wave) formation [8]. Recently, we have grown single-crystalline samples of the tetragonal  $\text{Lu}_5\text{Ir}_4\text{Si}_{10}$  ( $P4/mbm$ ). Unlike the above mentioned chain or layered compounds,  $\text{Lu}_5\text{Ir}_4\text{Si}_{10}$  is an intermetallic compound with nearly 3D structure, and yet it undergoes a strongly coupled commensurate CDW transition with  $q$  vector  $(0, 0, 3/7)$ . The CDW coexists with weak-coupled (BCS) superconductivity below 3.9 K [11].

In this Letter, we present the first observation of a combined commensurate structural transition and incommensurate CDW (155 K) that locks into a purely commensurate state at lower temperatures (55 K), and local-moment antiferromagnetism (below 2.8 K) in high-quality  $\text{Er}_5\text{Ir}_4\text{Si}_{10}$  single crystals which are isostructural to  $\text{Lu}_5\text{Ir}_4\text{Si}_{10}$ . As opposed to earlier canonical CDW systems [1–5], the anomalies of the bulk properties at the 155 K CDW transition are much sharper in  $\text{Er}_5\text{Ir}_4\text{Si}_{10}$ . Thus, we believe that  $\text{Er}_5\text{Ir}_4\text{Si}_{10}$  supplies a unique experimental example of a multiple phase transition system. The interplay of the  $f$  electrons of the local moment magnetism with the conduction electrons involved in the CDW transitions, together with the structural transformation, makes this metallic system a paradigm for both experimental and theoretical study.

Two single-crystal samples of  $\text{Er}_5\text{Ir}_4\text{Si}_{10}$  have been synthesized in a triarc crystal puller using the Czochralski technique described elsewhere [12] (pulling rate 5 mm/h; seed rotation 20 rpm). The purity of the elements (melted in a stoichiometric ratio) was Er:4N, Ir:4N, and Si:5N. The crystals were analyzed using electron-probe microanalysis which proved them to be single phase (secondary phases <1%) and to have the correct 5:4:10 stoichiometry (within 2% resolution). Powder x-ray diffraction measurements

showed that the samples have a tetragonal structure (see Fig. 1) and the lattice parameters are  $a = 12.543(1)$  Å and  $c = 4.203(1)$  Å. The single-crystalline nature of the samples was verified using a Laue diffraction technique. For transport and magnetization measurements small bars have been cut by spark erosion from the oriented crystals. The magnetic susceptibility ( $\chi$ ) was measured, from 1.8 to 300 K, using a Quantum Design magnetometer (magnetic property measurement system) while the resistivity ( $\rho$ ) and specific heat ( $C_p$ ) (1.8 to 300 K) were measured using a Quantum Design physical property measurement system. The high-resolution x-ray measurements were performed with synchrotron radiation ( $\lambda = 0.400$  Å) at beam line D3 of Hasylab at DESY in Hamburg, Germany.

$\text{Er}_5\text{Ir}_4\text{Si}_{10}$  adopts the  $\text{Sc}_5\text{Co}_4\text{Si}_{10}$ -type structure ( $P4/mbm$ ) [13]. Three crystallographically independent Er atoms are present in the unit cell, as shown in Fig. 1. The Er1 atoms form a chainlike structure along the  $c$  axis that is embedded in a network of closely bonded Er2, Er3, and Ir atoms. Most probably, the Er1 chains form the quasi-1D electron band.

Figure 2 shows the temperature dependence of the resistivity between 1.8 and 300 K along the  $a$  and  $c$  axes. An abrupt increase in  $\rho$  is observed at  $\approx 155$  K which, upon further cooling, develops into a plateau and drops sharply around 55 K. The dramatic changes in  $\rho(T)$  clearly elucidate the presence of two transitions at 155 and 55 K. The pronounced hysteresis observed between 40 and 120 K establishes the *first-order* character of the 55 K transition. Note that the anisotropy in the resistivity is quite small ( $\rho_a/\rho_c \sim 2.4$ ). This ratio is indeed much less than that observed in canonical CDW systems, such as  $\text{NbSe}_3$  [2]: Low anisotropy indicates strong interchain coupling. The behavior of  $\rho(T)$  could be understood in terms of two conducting channels, one related to the Er1 sites and the other due to the Er2-Er3 network. The first channel undergoes a metal-insulator transition at 155 K while the networks

have finite conductivity that remains at all temperatures. Below the lock-in transition ( $T < 55$  K), the commensurate modulation destroys the perfect nesting and  $\rho$  suddenly drops at this temperature.

The magnetic susceptibility  $\chi(T)$  obeys a simple Curie-Weiss law from 20 to 300 K with an effective local moment of  $\mu_{\text{eff}} = 9.7\mu_B$  and a Curie-Weiss temperature  $\theta_p = -3.0$  K (data not shown). No anomaly is found at the temperatures of the CDW transitions. This is explained by the large local moment contribution to the susceptibility that overwhelms any changes in the Pauli paramagnetism such as were observed in  $\text{Lu}_5\text{Ir}_4\text{Si}_{10}$  [11]. The low temperature susceptibility data exhibit a peak at 2.8 K, thereby establishing the antiferromagnetic ordering of  $\text{Er}^{3+}$  moments below this temperature.

Figure 3 presents the specific-heat data between 2 and 160 K of the same crystal. A huge peak in the specific heat ( $\Delta C_p \sim 160$  J/mol K) is observed at 145 K (see upper inset of Fig. 3), while no anomaly is found at the lower transition (55 K). The sharp ( $\Delta T/T_{\text{CDW}} \sim 3\%$ ) upper transition is accompanied by a large entropy change of  $0.3R$  where  $R$  is the gas constant. This suggests *strong electron-phonon coupling* in this phase transition which could arise due to a contribution from phonon softening that results in a Kohn anomaly [6]. In our earlier work we have established the occurrence of such a strong coupling CDW in the isostructural compound  $\text{Lu}_5\text{Ir}_4\text{Si}_{10}$  [11] where the gap is estimated to be around 700 K indicating that the actual phase transition is suppressed well below the mean-field value. A similar scenario is very likely applicable to  $\text{Er}_5\text{Ir}_4\text{Si}_{10}$ . The sharp ( $\Delta C_p \sim 10$  J/mol K) specific-heat anomaly at 2.8 K, shown in the lower inset of Fig. 3, reflects the bulk nature of the magnetic transition. Moreover, the transition could be easily suppressed by applying a magnetic field of 1 T (data not shown).

High-resolution x-ray diffraction on a small homogeneous piece of single crystal was performed with synchrotron radiation for temperatures between 10 and 300 K.

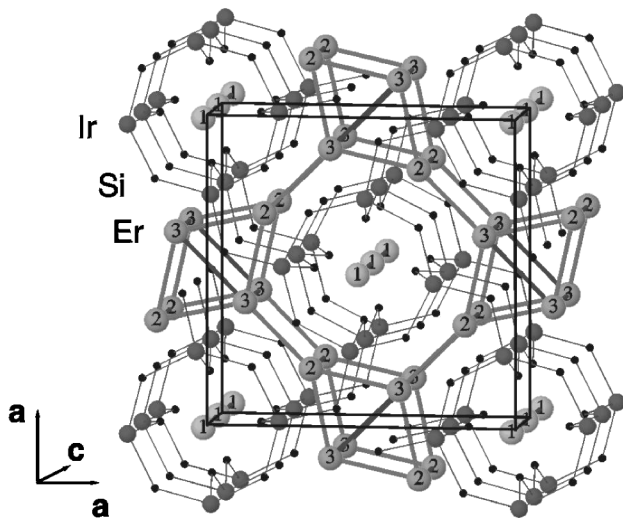


FIG. 1. Crystal structure of  $\text{Er}_5\text{Ir}_4\text{Si}_{10}$  (space group  $P4/mbm$ ).

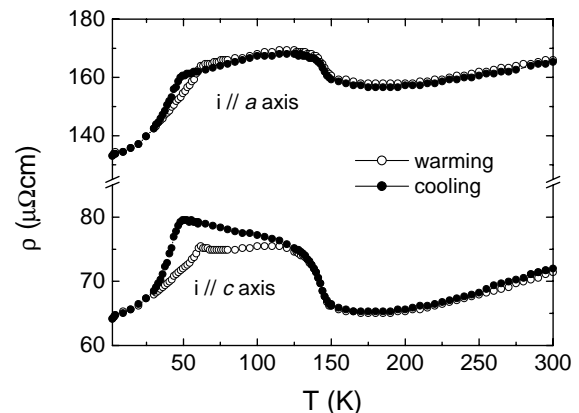


FIG. 2. Temperature dependence of the resistivity ( $\rho$ ) with current along  $a$  and  $b$  axes from 1.8 to 300 K. The sharp jumps reflect the two CDW transitions as explained in the text.

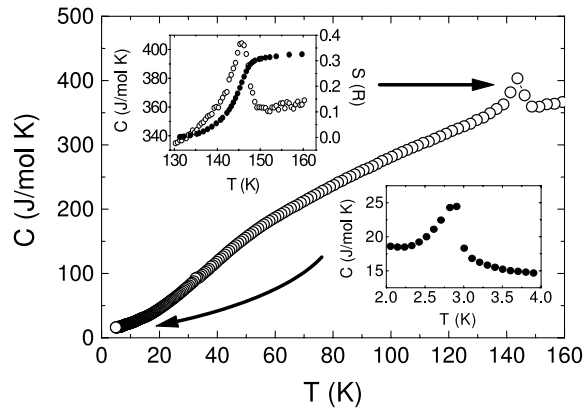


FIG. 3. Temperature dependence of the specific heat ( $C_p$ ) from 2 to 160 K. The upper inset shows the behavior of  $C_p$  at the upper CDW transition and the entropy estimated after the background subtraction. The lower inset displays the specific-heat data below 4 K.

Below  $T_{CDW} = 155$  K, five superlattice reflections start to develop along  $c^*$  between consecutive Bragg reflections. Upon cooling, the intensities of these reflections grow, and hysteresis was not observed, suggesting a *second-order* transition at 155 K (Fig. 4). In accordance with this interpretation, the temperature dependence of the intensities of the superlattice reflections is roughly proportional to  $(T_{CDW} - T)^{1/2}$ . However, because of the limited number of data points, our experiment does not allow an accu-

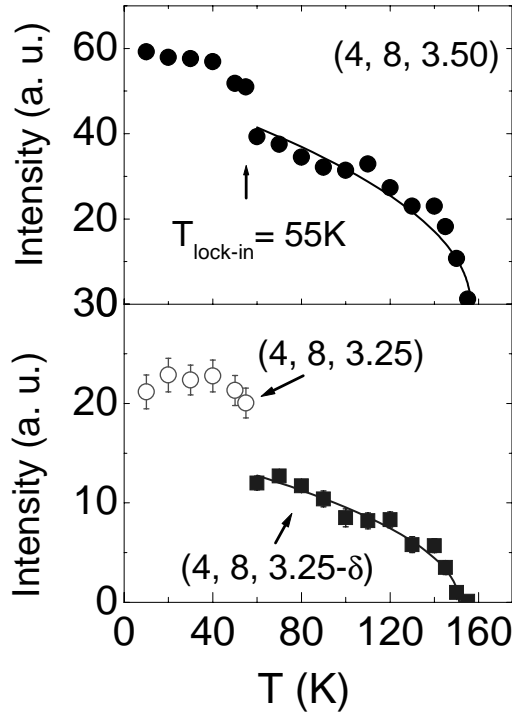


FIG. 4. Intensities vs temperature for the satellite reflections  $(4, 8, 3.50)$ ,  $(4, 8, 3.25 - \delta)$  and half of the intensity of  $(4, 8, 3.25)$  [ $(4, 8, 3.25 + \delta)$  not shown] from a  $\omega$  scan. The lines show a  $(T_{CDW} - T)^{1/2}$  dependence.

rate determination of the critical exponent. The positions of these reflections can be described by modulation wave vectors  $q_1 = (0, 0, 1/4 - \delta)$ ,  $q_2 = (0, 0, 1/4 + \delta)$ , and  $q_3 = (0, 0, 1/2)$ . Figure 5 illustrates the development of the incommensurate peaks beginning at 155 K and merging into a commensurate  $q = (0, 0, 1/4)$  single peak at 55 K. The inset of Fig. 5 displays the “incommensurability”  $\delta$  which clearly varies continuously with temperature, thus indicating a truly incommensurate CDW state. At 55 K a lock-in transition is observed, whereby  $\delta$  jumps to zero, and a fourfold superstructure results. The lock-in transition is seen as a small increase of the intensity of the  $(0, 0, 1/2)$  satellite, as shown in the upper plot of Fig. 4. Furthermore, the intensity of the  $(0, 0, 1/4)$  satellite ( $\delta = 0$ ), as found from the  $\omega$ -scan experiment, just below  $T_{lock-in}$  is approximately equal to the sum of the intensities of the corresponding incommensurate satellites at  $(0, 0, 1/4 \pm \delta)$  just above  $T_{lock-in}$ .

The simultaneous development of incommensurate and commensurate modulations makes  $\text{Er}_5\text{Ir}_4\text{Si}_{10}$  an atypical CDW system. Two scenarios can be envisaged to explain this feature. In the first, it is assumed that at  $T_{CDW}$  the unit cell doubles. The Fermi surface is modified accordingly, and allows nesting, resulting in a 1D-incommensurate CDW where  $q_{1D} = (0, 0, 1/2 - 2\delta)$  with respect to the doubled unit cell. In the second scenario, it is assumed that the Fermi surface permits nesting with both  $(0, 0, 1/4 \pm \delta)$  and a 2D-incommensurate CDW develops. The interactions between the two distortions are then responsible for the distortion with  $q_3 = q_1 + q_2$ . In favor of the first scenario is that it involves only a 1D CDW, whereas, for the second hypothesis, two independent nesting conditions are required with fortuitous relation  $(1/4 \pm \delta)$ . The symmetry  $P4/mbm$  cannot be responsible for two nesting conditions along  $c^*$  that are symmetry

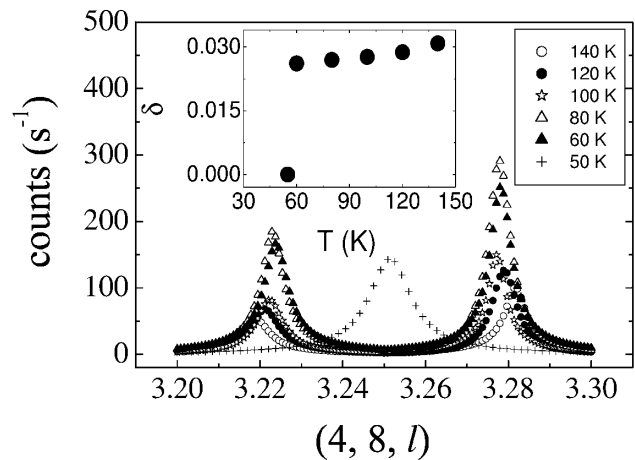


FIG. 5. Temperature dependence of the  $Q$ -scan x-ray reflections  $(4, 8, [3.20, \dots, 3.30])$ . The two peaks coming from the incommensurate component merge into a single peak in the commensurate state at 55 K. The inset shows the temperature dependence of the incommensurability  $\delta$  (as defined in the text).

related. We note that a transition towards a structure with a doubled  $c$  axis is possible via a second-order phase transition [14]. Therefore, we propose the first scenario to explain the observations: At  $T_{\text{CDW}} = 155$  K, a second-order, structural phase transition occurs. The modified electronic structure then induces the CDW transition, whereby the order parameter of the CDW grows in concert with the order parameter of the structural transition. The CDW state might be favored in the doubled unit cell by a better nesting condition or by an increased electron-phonon coupling.

Polycrystalline and single-crystal neutron data suggest the presence of a large magnetic moment on the Er1 site and smaller ones on Er2 and Er3 sites, below 2.8 K [15]. The presence and interaction of local moments in this material classify  $\text{Er}_5\text{Ir}_4\text{Si}_{10}$  as the *first intermetallic CDW system with local moment ordering* [16]. It is also interesting to note that the anisotropy in  $\chi$  increases below 20 K, probably signifying the additional effects of crystal electrical field.

Although it is possible to understand the behaviors of  $\rho$  and  $\chi$  within the CDW and local-moment pictures, the large peak in the  $C_p$  at 145 K denotes this CDW transition as an unusual one, unlike conventional CDW systems where the anomalies in the bulk properties are quite weak at the transition. It is generally believed that defects tend to wipe out the sharp anomaly in conventional CDW compounds. In stoichiometric single-crystal  $\text{Er}_5\text{Ir}_4\text{Si}_{10}$ , we expect that the influence of defects will be much smaller making this system essentially disorder free. One does not observe any anomaly in  $C_p$  around 55 K since it is a lock-in transition, which probably involves very small entropy change but a large change in the resistivity due to the decrease of the energy gap.

In conclusion, we have established that  $\text{Er}_5\text{Ir}_4\text{Si}_{10}$  exhibits multiple CDW transitions (1D incommensurate at 155 K and lock-in at 55 K) and a transition towards a magnetically ordered state at 2.8 K. We speculate that the magnetic moments of the Er atoms play a definite role in these transitions and further understanding requires band structure calculations to determine the possible nesting and gapping of the Fermi surface which leads to the CDW transitions. Finally, we stress that the series of  $\text{RE}_5\text{Ir}_4\text{Si}_{10}$  compounds offer a new and extremely convenient paradigm with which to study strongly coupled CDW and co-existing superconductivity or magnetism.

The crystals were grown at FOM-ALMOS under the supervision of Dr. A. A. Menovsky. Part of this research is supported by the Dutch Foundation FOM and the Deutsche Forschungsgemeinschaft (DFG). We acknowl-

edge H. G. Krane for assistance with the synchrotron radiation experiment.

---

\*Permanent address: Graduate School of Science, Osaka University, Toyonaka, 560-0043, Japan.

- [1] J. A. Wilson, F. J. Di Salvo, and S. Mahajan, *Adv. Phys.* **24**, 117 (1971).
- [2] N. P. Ong and P. Monceau, *Phys. Rev. B* **16**, 3433 (1977); N. P. Ong and J. W. Brill, *Phys. Rev. B* **18**, 5265 (1978).
- [3] J. P. Pouget, *Low-Dimensional Electronic Properties of Molybdenum Bronzes and Oxides*, edited by C. Schlenker (Kulwer Academic Publishers, Dordrecht, The Netherlands, 1989), p. 87.
- [4] G. Gruner, *Rev. Mod. Phys.* **60**, 1129 (1988); *Charge Density Waves in Solids* (Addison-Wesley, Reading, MA, 1994).
- [5] L. B. Coleman, M. J. Cohen, D. J. Sandman, F. G. Yamagishi, A. F. Garito, and A. J. Heger, *Solid State Commun.* **12**, 1125 (1973).
- [6] D. E. Moncton, J. D. Axe, and F. J. DiSalvo, *Phys. Rev. Lett.* **34**, 734 (1975).
- [7] W. L. McMillan, *Phys. Rev. B* **16**, 643 (1977). See also C. M. Varma and A. L. Simons, *Phys. Rev. Lett.* **51**, 138 (1983).
- [8] R. N. Shelton, L. S. Hausermann-Berg, P. Klavins, H. D. Yang, M. S. Anderson, and C. A. Swenson, *Phys. Rev. B* **34**, 4590 (1986).
- [9] H. D. Yang, P. Klavins, and R. N. Shelton, *Phys. Rev. B* **43**, 7688 (1991).
- [10] K. Ghosh, S. Ramakrishnan, and Girish Chandra, *Phys. Rev. B* **48**, 4152 (1993).
- [11] B. Becker, N. G. Patil, S. Ramakrishnan, A. A. Menovsky, G. J. Nieuwenhuys, J. A. Mydosh, M. Kohgi, and K. Iwasa, *Phys. Rev. B* **59**, 7266 (1999).
- [12] A. A. Menovsky and J. J. M. Franse, *J. Cryst. Growth* **65**, 286 (1983).
- [13] H. F. Braun, *J. Less-Common Met.* **100**, 105 (1984); H. F. Braun, K. Yvon, and R. Braun, *Acta Crystallogr. Sect. B* **36**, 2397 (1980).
- [14] H. T. Stokes and D. M. Hatch, *Isotropy Subgroups of the 230 Crystallographic Space Groups* (World Scientific, Singapore, 1988), Table I, p. 1–146.
- [15] F. Galli, R. Feyerherm, S. Ramakrishnan, G. J. Nieuwenhuys, and J. A. Mydosh (to be published).
- [16] Very recently dissimilarities were drawn between conventional CDW systems, e.g.,  $\text{TaSe}_2$  [R. M. Fleming, D. E. Moncton, D. B. McWhan, and F. J. Di Salvo, *Phys. Rev. Lett.* **45**, 576 (1980)], and the charge-ordered perovskite manganites [C. H. Chen, S. Mori, and S.-W. Cheong, *Phys. Rev. Lett.* **83**, 4792 (1999)]. It would be particularly interesting to contrast the charge and spin orderings in  $\text{RE}_5\text{Ir}_4\text{Si}_{10}$  with these latter oxides.